HIGH PERFORMANCE ANTIFOULING/ANTICORROSION COATINGS FOR PROTECTING CARBON STEEL AND LOW ALLOYING STAINLESS STEEL HEAT EXCHANGERS IN LOW ENTHALPY GEOTHERMAL FLUIDS

*R. Losada[1], S. Holberg[2], L. Freire[3] and J. Van Bael[4]

[1] Danish Technological Institute, Kongsvang Allé 29, 8000 Aarhus C, Denmark (rlm@teknologisk.dk)
[2] University of Wyoming, 1000 E University Ave., Laramie, WY 82071, USA
[2] AIMEN Technology Center, Relva 27A, 36410 O Porriño, Spain
[3] VITO Flemish Institute for Technological Research, Mol, Belgium

ABSTRACT

Geothermal energy is an important and increasing energy segment. The heat exchangers transferring heat from the geothermal brine to the working fluid are the most critical installations and represent a major share of the total cost. Geothermal brines create very aggressive environments and corrosion and fouling are major issues. Today, heat exchangers are usually constructed of resistant but costly materials like Inconel or Titanium. In the presented study, which was carried out in the frame of the European H2020 project MATChING, we investigated economic materials like carbon or standard stainless steels in combination with cost-effective, protective coatings by laboratory immersion tests. Some of the tested combinations pass all laboratory requirements and are promising economic alternatives for heat exchangers in geothermal installations.

INTRODUCTION

Geothermal energy has a lower environmental footprint than any other renewable energy source, and both, the European Council and the European Parliament recognize geothermal energy's essential role in the European energy transition towards net-zero greenhouse gas emissions by 2050. Recent estimates indicate that the global production capacity for geothermal electricity is at about 13.3 GW (installed capacity in January 2016) and is expected to reach about 18.4 GW by 2021 [1]. The economic feasibility of geothermal installations relies on continuous operation of the geothermal loop. To be competitive and reduce costs operators must pay attention to proper maintenance of critical equipment, especially heat exchangers transferring heat from the geothermal fluid to the working fluid.

Corrosion and scaling are the major issues in the exploitation of geothermal sources. Geothermal fluids are complex mixtures consisting of gases dissolved in high salinity solutions, which create very aggressive environments. The effects on the elements of the installation in direct contact with the brines, especially heat exchangers, can be minimized by use of resistant materials such as superduplex, inconels, hestealloys or Ti alloys. Those materials perform well in terms of corrosion resistance, but they are very expensive. Moreover, some of those exotic materials are especially prone to induce scaling and have mechanical restrictions, i.e. limited machinability compared to carbon steel. Given these considerations, it is desirable to find alternative materials for heat exchangers that can overcome these disadvantages and acquire comparable heat exchange.

Herein, we present laboratory activities conducted to identify adequate coating solutions for protecting heat exchanger tubes made of economic carbon steel and low alloying stainless steel against corrosion and fouling caused by the geothermal brines. The selected carbon steel EN 10028:2 P265G is a common material for high temperature and pressure equipment, such as pressure vessels or boilers. The selected stainless steel AISI 316 L is an austenitic steel widely known for its excellent corrosion resistance and relatively low price. For a cost comparison among the selected materials and other alloys see Table 1 [2,3].

Table 1: Cost ratio for different materials

	Metals	Pitting Resistance equiv. %	Cost (relative to steel)
Carbon steel	P265G, L80, N80	-	1
Stainless steels & Alloys	316L	27	8.3
	318LN	34	7.1
	904L	36	19.4
	2507	41	12.6
	Alloy 31	52	33

As cost-effective coatings, combinations of existing commercial coating solutions from various providers with good track records were considered,

including a top coat developed at the Danish Technological Institute.

Chemistry of geothermal fluids and material solutions depend on the local geology. The present work, carried out in the frame of the MATChING project [4], focused on the geothermal site of Balmatt (Belgium). The anticorrosion performance and surface properties of the coatings have been investigated at laboratory scale in conditions that mimic real operational conditions but without flow factor. The heat transference across the coatings was estimated in order to evaluate the impact of the coating on the heat transfer efficiency.

EXPERIMENTAL

Materials and Coatings

As base material, carbon steel EN 10028:2 P265G and stainless steel AISI 316 L were selected. Five coatings were selected

F1: Commercial, non-stick fluoropolymer coating (either PTFE (polytetrafluoroethylene), FEP (fluorinated ethylene propylene) or PFA (perfluoroalkoxy) with pigments/fillers, may comprise a primer. Curing temperature > 300 °C.

F2: Like F1, but specifically marketed for corrosion protection.

Ph: Phenolic resin-based, one-component coating with fillers/pigments, heat cured (Temperature not disclosed), number of layers not disclosed. Marketed for severe corrosion protection, maximum service temperature 180°C.

EP1: Multilayer coating where sequence and thicknesses were optimized to provide an optimal compromise of corrosion protection, repellent properties and thermal resistance. Layers 1 and 2 are typically cured at ambient temperature and marketed as corrosion protection for infrastructure (for example steel bridges) that is permanently immersed in water. Layer 1 is a commercial zinc-rich, two-component epoxy primer, cured at room temperature. Layer 2 is a commercial, amine-cured, two-component epoxy coating with fillers/pigments, including iron mica as barrier pigment, cured at 60°C. Layer 3 is applied to obtain a smoother surface and is a commercial, amine-cured, two component epoxy top coat with fillers/pigments, cured at 60°C. Layer 4 is applied to obtain a low surface energy and is a hybrid organic-inorganic sol-gel coating developed at DTI similar to the described in references [5, 6], cured at 185°C (thus all layers were heated to 185°C).

EP2 is equal to EP1 except that layer 1 is missing.

The coatings' providers recommended each of the coatings based on the knowledge that the application environment would be aggressive and erosive. The general coating characteristics are described hereafter in Table 2. All coatings provide a low surface tension σ. Measuring solely the non-polar part of the surface tension by hydrocarbon test inks (TIGRES Dr Gerstenberg GmbH, 24-45 mN/m), F1, F2, EP1 and EP2 provide σ <24 mN/m, Ph provides σ = 30 mN/m. Measuring both polar and non-polar part according to DIN ISO 8296 with ethanol-water test inks (Plasmatreat, Series C, surface tensions 30-72 mN/m), F1, F2, EP1 and EP2 provide σ < 30 mN/m. We refrain from giving trade names of the commercial coating systems as it could be misunderstood as a commercial promotion.

Table 2: General coating characteristics

Coating	Type	Substrate	Dry film thickness (µm)
F1	Fluoropolymer based	both	75
F2	Fluoropolymer based	both	100-120
Ph	Phenolic based	both	250-270
EP1	Composite epoxy/sol-gel coating	P265G	250-300
EP2	Composite epoxy/sol-gel coating	AISI 316L	150

Testing Strategy

The best material performance test is conducted in the environment of the intended use. However, appropriate tests in simulated laboratory environments with simplified set-ups can produce very valuable information. Accordingly, we used a custom-designed autoclave-like system, called "LOTU", in conjunction with different characterization techniques to assess the corrosion protection, chemical resistance and surface properties provided by the coatings. The geothermal fluid found in Balmatt is a brine with up to 165 g/l total dissolved solids and the major constituents are sodium and chlorine, which account for 90% of the dissolved ions [7]. As testing media, we used a synthetic brine with the same composition as the brine found at Balmatt. The exact composition of the used synthetic brine can be found in Table 3.

Table 3: Composition of the synthetic brine

Cl	Na	K	Ca	HNO_3
94.0 g/l	50.1 g/l	3.3 g/l	7.5 g/l	1.2 g/l
Fe	Mg	SO_4	pH	Conductivity
817 mg/l	495 mg/l	350 mg/l	5.55	177.7 µS/cm

LOTU test. Coated samples were mounted in a PEEK (polyether ether ketone) holder, positioned vertically and completely immersed in the synthetic brine within a 0.750 L pressure vessel. The samples

were not in contact with each other and a stirrer ensured homogeneous mixing and incorporated flow dynamics. A pressure controller valve is connected to the vessel and enables in-situ monitoring of the pressure inside. The test duration was 570 h (24 days). The dimensions of the test specimens were 50×50×5 mm and they were coated on all sides. The testing conditions are detailed in Table 4.

Table 4: Conditions at the LOTU test and in situ at Balmatt

	LOTU	In situ Balmatt	
Temperature (°C)	130	125-130	
Pressure (Bar)	40	~40	
Partial pressure of CO_2	-	CO_2 in the gas mixture	76,5 Vol. %
pH	5.55	~5.50	
Stirring (rpm)	600	Flow velocity	1 m/s
Time (h)	~570		

Coating Evaluation. Dry film thickness (DFT) was measured on flat samples by induction/eddy current probe (Bykotest 7500, Byk-Gardener), The performance and integrity of the coatings after exposure to the LOTU was assessed visually (rusting, blistering), by testing adhesion, and by electrochemical impedance spectroscopy (EIS), see Table 5.

Table 5: Success criterion for adhesion, blistering and rusting after exposure.

Parameter	Standard	Acceptance criterion
Adhesion	ISO2409:2007 (thickness<250 µm), ASTM D 3359-02 (thickness >250 µm).	Rating 1 or less
Blistering	ASTM D714-02.	Rating 8F or no blisters
Rusting	ISO 4628-3.	Surface free of rusting (rating 0)

EIS measurements were obtained using a potentiostat PGSTAT20 AUTOLAB from Ecochemie®. The EIS analysis was performed in the synthetic brines, at room temperature, and under aerated conditions, therefore atmospheric oxygen could have access to the metal surface through the pervious coating, accelerating the corrosion process.

The electrode impedance was measured in the frequency range between 100 kHz and 0.1 Hz (5 points per decade) with an AC potential perturbation of 200 mV (rms) amplitude. The working electrode was the coated sample, and the exposed surface was 1 cm^2, a platinum mesh was the auxiliary (counter) electrode and the reference electrode was a platinum wire. The auxiliary electrode and the reference electrode were short-circuited to obtain more accurate measurements. All electrochemical tests were performed using a vertical cell filled with 50 mL of the synthetic brine. The measurements were carried out under continuous stirring. The performance of the coatings was evaluated from the magnitude of the impedance modulus |Z| at low frequency.

RESULTS AND DISCUSSION

Macroscopic characterization after exposure

Immediately upon removal from the LOTU, the coatings were visually assessed and rated for blistering, rusting and adhesion. Results are presented in Tables 6, 7.

For carbon steel, coatings F1 and F2 present many little blisters homogeneously distributed along the sample. They both also showed rust patches on the surface and coating F1 failed in adhesion. Contrary, coatings Ph and EP1 do not show visible defects and retain excellent adhesion. For stainless steel, all tested coatings (F1, F2, Ph and EP2) show no damages and excellent adhesion.

For all samples meeting the acceptance criteria, the surface remains very smooth and the surface energy values very low except for coating Ph, whose surface energy rises from 30 to 44 mN/m. Smoothness and low surface energy are key aspects in heat exchangers for reducing tube wall friction and improving the overall heat transference. According to literature, 70% of the total heat transfer resistance across a heat exchanger tube is the slow-moving fluid coming into contact with the tube wall [8].

Table 6: Results from the physical characterization for the coatings on P265G after the exposure tests at LOTU.

Coating	F1	F2	Ph	EP1
Adhesion rating	5	0	0	0
σ (mN/m)	-	-	44	25
Blister	6 MD	6 M	None	None
Rust	3	3	0	0
Comment	Failed	Failed	Pass	Pass

Table 7: Results from the macroscopic characterization for the coatings on AISI 316 after the exposure tests at LOTU.

Coating	F1	F2	Ph	EP2
Adhesion rating	0	0	0	0
σ (mN/m)	<24	<24	44	25
Blister	None	None	None	None
Rust	0	0	0	0
Comment	Pass	Pass	Pass	Pass

Electrochemical Impedance Spectroscopy (EIS)

Following the macroscopic evaluation, the samples that met the acceptance criteria were further assessed by means of EIS. Contrary to classic macroscopic evaluation techniques, which are based on subjective judgement, EIS can quantify the protective character of the coatings measuring objective data. In this study, we used the impedance modulus (|Z|) at low frequencies (0.1 Hz) [9] as a quantitative parameter to compare the protective properties of the coatings [10,11]. The following criterion was applied [12,13]; coatings with $|Z|_{0.1Hz}$ >10^8 $\Omega \cdot cm^2$ provide excellent protection without noticeable penetration of electrolyte. Coatings with $|Z|_{0.1Hz}$ between $10^7 \Omega \cdot cm^2$ and 10^8 $\Omega \cdot cm^2$ provide good protection with minimal electrolyte absorption into the coating. $|Z|_{0.1Hz}$ >10^6-10^7 $\Omega \cdot cm^2$, the electrolyte penetrates the coating and creates a path to the surface of the metal substrate, there is not active corrosion yet and the degree of protection is ranked as doubtful. $|Z|_{0.1Hz}$ <10^6 $\Omega \cdot cm^2$, the coating is deemed as non-protective, the electrolyte penetrates the coating and there is active corrosion process at the metal surface. Figure 1, presents the |Z|0.1Hz values for the tested coatings

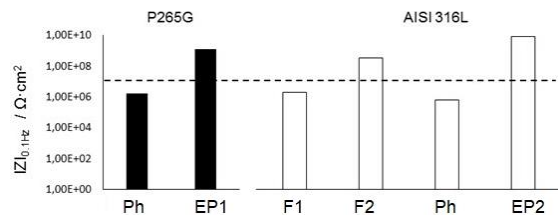Figure 1: Values of |Z|0.1Hz for the different coatings after exposure. The dashed line is set at 10^7 $\Omega \cdot cm^2$ which is the limit for a coating to be ranked as protective.

Coatings EP1 on carbon steel and F2 and EP2 on stainless steel have the highest values of $|Z|_{0.1Hz}$, they are in the range of 10^8 $\Omega \cdot cm^2$, which indicates a remarkable capacity to withstand the penetration of electrolytes. Contrary, coatings Ph and F1 present values of $|Z|_{0.1Hz}$ below 10^6 $\Omega \cdot cm^2$, suggesting that, the electrolyte has reached the metal substrate, though there are not visible evidences of corrosion yet, the sensitivity of EIS allows to detect the corrosion processes before visible damage occurs.

Thermal Transfer Resistance

The thermal resistance factor introduced by the best performing coatings F2, EP1 and EP2 was calculated using equation (1).

$$Rf = \frac{d_f}{k_f} \qquad (1)$$

Rf is the thermal resistance on a specific side of the heat exchanger (m^2 K/W), d_f is the average thickness of the coating layer (m) and *kf* is the thermal conductivity of the coating (W/m·K).

The thermal conductivity of the coatings (*kf*) was estimated using equation (2) and data in literature [14,15,16,17,18].

$$k_f = \frac{x_1 + x_2 + \cdots x_i}{\frac{x_1}{k_1} + \frac{x_2}{k_2} + \cdots \frac{x_i}{k_i}} \qquad (2)$$

kf is the thermal conductivity of the coating, $x_1 \ldots x_i$ are the thicknesses of the different layers and $k_1 \ldots k_i$ their respective thermal conductivities.

The heat transfer resistance data is summarized in Table 8.

Table 8: Heat transfer resistance of the different coatings

Coat.	Thickness* (µm)	Thermal conductivity (W/m K)	Thermal resistance (m^2K/W)
F2	100	~ 0.25	0.0004
EP1	250	~ 0.63	0.0004
EP2	150	~ 0.58	0.00025

* For calculations were used the lowest values of the thickness ranges presented in table 2

In Balmatt the heat exchangers are made of high alloying stainless steels and were designed with a fouling factor in the brine side (*Rf*) of 0.0004 m²K/W. Through the results presented in table 6, it can be understood that, the coatings impact the thermal conductivity by a lower or similar factor than the design *Rf*. Moreover, the coatings prevent corrosion and the fouling situation is likely to be improved.

CONCLUSIONS

Different coatings were tested to evaluate their potential application on heat exchangers tubes made of low alloying stainless steel and carbon steel in geothermal applications. Results indicate that some of the tested coatings, EP1 on carbon steel and F2 and EP2 on stainless steel effectively protect against corrosion, have limited impact on the heat transfer resistance, and provide adequate surface properties (smoothness and low surface energy). The results are promising for lowering the capital and maintenance cost of brine heat exchangers in geothermal installations as they are based on existing commercial coatings. The question to be raised now is, whether the coatings can be applied defect free on a larger installation and whether the laboratory tests conducted in a static fluid, correlate well with the field performance under flowing conditions. A currently ongoing test at the Balmatt installation shall answer these questions.

NOMENCLATURE

σ   Surface energy, mN/m
|Z| Impedance modulus, $\Omega \cdot cm^2$
Rf   Thermal resistance factor, m^2 K/W
d_f Average coating thickness, m

kf Thermal conductivity, W/m·K
x_i Average thicknesses of coating layers, m
k_i Thermal conductivities coating layers, W/m·K

AKNOWLEDGEMENTS

REFERENCES

[1] Matek, B. 2016 Annual US & Global Geothermal Power Production Report. Geothermal Energy Association (2016).URL http://geoenergy.org/reports/2016/2016%20Annual%20US%20Global%20Geothermal%20Power%20Production.pdf (accessed 02.01.2019)

[2] Mundhenk, N., Huttenloch, P., Kohl, T., Steger, H., Zorn, R. Laboratory in-situ corrosion studies in geothermal environments. GRC transactions 36, pp. 1101-1106, 2012.

[3] http://www.steeltank.com/Portals/0/Pressure%20Vessels/SSWseminarOct2012/Relative%20Cost%204%2015%202012.pdf (accessed 20.12.2018)

[4] http://matching-project.eu/

[5] Bischoff, C., Holberg, S. ''Repellent coating composition and coating method for making and uses thereof.'' WO 2012/ 083970 A1, 2012.

[6] Losada, R., Holberg, S., Bennedsen, J.M.D., Kamuk, K., Nielsen, F. Coatings to prevent frost. J Coat Technol Res 13(4), pp. 645-653, 2016.

[7] Laenen, B., Boss, S. Development of the first deep geothermal doublet in the Campine Basin of Belgium. European Geologist, 43, pp. 16-20, 2017.

[8] Curran, E.L. Solving heat exchanger tube problems with thin film thermally conductive coating applications and novel tube and pipe cleaning as precursor to coating application and NDT. Proceedings of the International Conference on Heat Exchanger Fouling and Cleaning VIII, 2009.

[9] O'Donoghue, M., Garret, R., Garret, J., Graham, R., Datta, V.J., Gray, L.G.S., Drader, B. Field perfromance versus laboratory testing: a study of epoxy tank and vessel linings used in the Canadian oil patch. Paper 03051 Corrosion 2003.

[10] Chen, Y., Wang, X.H., Li, J., Lu, J.L., Wang, F.S. Long term anticorrosion behavior of polyaniline on mild steel. Corr. Sci. 49, pp. 3052-3063, 2007.

[11] Loveday, D., Peterson, P., Rodgers, B. Evaluating organic coatings with electrochemical impedance spectroscopy. Part 3: Protocols for testing coating with EIS. JCT Coatings Tech, pp. 22-27, 2005.

[12] Bierwagen, G.P., He, L., Li, J., Ellingson, L., Tallman, D.E. Studies of new accelerated evaluation method for coating corrosion resistance-thermal cyclic testing. Prog. Org. Coat. 39, pp.67-78, 2000.

[13] Shi, A., Koka, S., Ullet, J. Performance evaluation on the weathering resistance of two USAF coating systems (standard 85285 topcoat versus fluorinated APC topcoat) via electrochemical impedance spectroscopy. Prog Org Coat 52, pp. 196-209, 2005.

[14] Velardo, J., Singh, R., Date, A., Date, A. An investigation into the effective thermal conductivity of vapour chamber heat spreaders. Energy Procedia 110, pp. 256-261, 2017.

[15] https://www.engineeringtoolbox.com/thermal-conductivity-d_429.html (Accessed 02.01.2019)

[16] Watson, T.W et al. Thermal conductivity of five epoxy resin specimens. National Bureau of Standards report, N 8574 (1964)

[17] Fu, Y-X. Thermal conductivity enhancement with different fillers for epoxy resin adhesives. Applied Thermal Engineering. 66, pp. 493-498, 2014.

[18] Holberg, S., Losada, R. Fouling-release coatings for steam condensers in thermal power plants. In H.U. Zettler (ed.), Heat Exchanger Fouling and Cleaning XII - 2017, Aranjuez (Madrid), Spain.